Flame Enhancement and Quenching in Fluid Flows

Natalia Vladimirova[†], Peter Constantin[‡], Alexander Kiselev[*], Oleg Ruchayskiy[†] and Leonid Ryzhik[‡]
[†] *ASCI/Flash Center, The University of Chicago, Chicago, IL 60637*
[‡] *Department of Mathematics, The University of Chicago, Chicago, IL 60637 and*
[*] *Department of Mathematics, University of Wisconsin, Madison, WI 53705*
(Dated: December 19, 2002)

We perform direct numerical simulations (DNS) of an advected scalar field which diffuses and reacts according to a nonlinear reaction law. The objective is to study how the bulk burning rate of the reaction is affected by an imposed flow. In particular, we are interested in comparing the numerical results with recently predicted analytical upper and lower bounds. We focus on reaction enhancement and quenching phenomena for two classes of imposed model flows with different geometries: periodic shear flow and cellular flow. We are primarily interested in the fast advection regime. We find that the bulk burning rate v in a shear flow satisfies $v \sim aU + b$ where U is the typical flow velocity and a is a constant depending on the relationship between the oscillation length scale of the flow and laminar front thickness. For cellular flow, we obtain $v \sim U^{1/4}$. We also study flame extinction (quenching) for an ignition-type reaction law and compactly supported initial data for the scalar field. We find that in a shear flow the flame of the size W can be typically quenched by a flow with amplitude $U \sim \alpha W$. The constant α depends on the geometry of the flow and tends to infinity if the flow profile has a plateau larger than a critical size. In a cellular flow, we find that the advection strength required for quenching is $U \sim W^4$ if the cell size is smaller than a critical value.

PACS numbers: PACS numbers: 47.70.Fw, 47.27.Te, 82.40.Py

I. INTRODUCTION

Turbulent combustion in premixed flows is a widely studied topic in both scientific and industrial settings (see e.g. [14, 39, 42]). The interest in the subject is due to an important influence that advection can have on the reaction process: both experimental [13, 47] and theoretical [3, 4, 17, 18, 23, 24, 33, 40, 50, 55] work shows that the propagation speed of the flame can be significantly altered by the fluid flow. Specifically, moderately intense levels of turbulence have the tendency to accelerate the flame speed v beyond its laminar value $v_\circ$. The mechanism and the extent of the flame acceleration depend on the particular regime of burning [12]. The general reason for the enhancement is that the fluid motion distorts the flame front, increasing the reaction area. On the other hand, if the advection is too strong, it can lead to the flame extinction. The critical strength of advection which leads to quenching depends on the extent of the flame, strength of reaction and diffusion, and properties of the flow.

At this stage, it is unreasonable to expect a complete analytical theory describing the process of combustion in a fluid phase. Indeed, detailed modelling of the phenomena involves solving a reaction-diffusion system involving temperature (or energy) and concentrations of reactants coupled with compressible Navier-Stokes equations describing motion of the mixture [39, 57]. Therefore, most of the studies in this field which seek analytical conclusions use heuristic reasoning or simplified models, which may approximately describe the system in certain combustion regimes. Some of the combustion regimes are relatively well-understood, such as the so-called flamelet regime, where flame thickness is small compared to the fluid velocity scales. The geometric optics approximation where the propagation of the front is ruled by Huygens principle is often used as a starting point in the analysis of this regime (see e.g. [34, 38]).

Our goal here is to study one of the most widely used PDE models of combustion, namely the scalar reaction-diffusion equation with passive advection:

$$\frac{\partial T}{\partial t} + \mathbf{u} \cdot \nabla T = \kappa \nabla^2 T + \frac{1}{\tau} R(T). \qquad (1)$$

Here T is the normalized temperature, $0 \le T \le 1$, $\mathbf{u}$ is the fluid velocity, which we assume is incompressible, κ is thermal diffusivity, and τ is the typical reaction time. In the absence of fluid velocity Eq. (1) admits flat propagation front with laminar burning velocity of the order of $v_\circ \sim \sqrt{\kappa/\tau}$ and characteristic thickness of the order of $\delta \sim \sqrt{\kappa\tau}$. The model (1) can be derived from a more complete system under assumptions of constant density and unity Lewis number (the ratio of material and temperature diffusivity), as shown, for instance, in [17]. The equation (1) has a more general applicability than the geometrical optics approximation; moreover, as we will discuss below, the geometrical optics limit can be obtained from (1) in a certain parameter range.

We will consider reaction rates $R(T)$ of two types, KPP (Kolmogorov, Petrovskii, Piskunov) [27, 36], and ignition. The KPP type is characterized by the condition that the function $R(T)$ is positive and convex on the interval $0 < T < 1$. This reaction type is used often in problems on population dynamics (see e.g. [5, 26]), but is relevant in combustion modelling, for example in some autocatalyctic reactions [28]. A reaction term of ignition type is characterized by the presence of critical ignition temperature, such that the function $R(T)$ is identically

zero below ignition temperature. This type of reaction term is used widely to model combustion processes (see e.g. [49, 57]), in particular approximating the behavior of Arrhenius-type chemical reactions which vanish rapidly as temperature approaches zero.

Our main goal is to gain insight into the question of how the geometry and the amplitude of the fluid flow influence the combustion process. Our study is partly motivated by recent analytical work [6, 19, 20, 29, 35] where rigorous bounds on combustion enhancement and quenching are proved. We test the sharpness of results in [6, 19, 20, 29, 35], and in addition derive new predictions. We consider two classes of flows. The first is shear flows, a representative of a wider class of flows, called "percolating" in [19], which have open streamlines connecting distant regions of the fluid. The second class is cellular flow, where the streamlines are closed and the flow consists of isolated cells. For each class of flows, we study both flame enhancement and quenching.

For flame enhancement study, we consider initial temperature in the form of the laminar front, with $T = 1$ in the semi-infinite region behind the front and $T = 0$ in the the semi-infinite region ahead of the front. Distorted by imposed flow, the flame front propagates as a travelling wave with velocity higher than laminar. The goal of the flame enhancement study is to obtain relations between flame propagation speed v and the properties of the flow, especially for the large advection velocities.

In the case of quenching phenomena, we consider initial temperature to be non-zero in a finite region. Since quenching cannot occur for the KPP-type source term [43, 44], we use the ignition-type reaction term. As shown by Kanel, there is a critical size $W_\circ$ of initial hot region below which the flame will be extinguished by diffusion alone, e.g. with no advection, when the temperature drops below the threshold and reaction ceases before the flame establishes a steady travelling wave configuration [32]. When advection is present, the fluid flow stretches the initially hot region so that it can be quenched by diffusion; hot regions of the size much larger than $W_\circ$ can be quenched in this manner. Our goal has been to understand how the geometry and amplitude of the flow influence the size of the band W of the initial hot region that can be quenched.

II. NUMERICAL SETUP AND METHOD

The simulation is set in two space dimensions, in a vertical strip of width L with periodic boundary conditions in x direction (Fig. 1). In reaction enhancement studies, the initial temperature was set to $T = 1$ in the lower half of the domain and to $T = 0$ in the upper half of the domain. In the quenching studies the initial temperature was set to $T = 1$ in a horizontal band of width W in the center of the domain, and to $T = 0$ elsewhere. The interfaces between hot and cold fluid were smoothed to match the laminar flame thickness.

We consider two types of flows, sinusoidal shear flow with amplitude U and wavelength L, perpendicular to the initial temperature front(s),

$$\mathbf{u} = U\left(0,\ \cos\frac{2\pi x}{L}\right), \tag{2}$$

and cellular flow with amplitude U and wavelength L,

$$\mathbf{u} = U\left(\sin\frac{2\pi x}{L}\cos\frac{2\pi y}{L},\ -\cos\frac{2\pi x}{L}\sin\frac{2\pi y}{L}\right). \tag{3}$$

In the quenching simulations, the size of the cell $L/2$ was a fraction of W, so that the initial band always contains integer number of cells.

Most of the reaction enhancement computations were done using KPP reaction rate [27, 36] in the advection-reaction-diffusion equation (1),

$$R(T) = \frac{1}{4}\,T(1-T), \tag{4}$$

with some of the simulations repeated with ignition type reaction,

$$R(T) = \frac{T_\circ}{(1-T_\circ)^2}\,(1-T), \qquad T > T_\circ, \tag{5}$$

where $T_\circ$ represents threshold temperature, below which $R(T) = 0$. In quenching studies we use ignition type reaction (5) with threshold temperature $T_\circ = 0.5$. Both reaction rates (4) and (5) were chosen to exactly match, in the absence of advection, laminar burning velocity $v_\circ = \sqrt{\kappa/\tau}$. The corresponding laminar flame thickness is in both cases of the order of $\delta = \sqrt{\kappa\tau}$; for KPP reaction it is several times wider than for ignition.

Equation (1) with reaction rates (4) and (5) has been solved using a fourth-order explicit finite difference scheme in space and a third-order Adams-Bashforth integration in time. The grid size was chosen so as to accurately represent the shear across the reacting region: typically of the order of 12 zones across the flame interface for thin fronts and at least 32 zones per period for

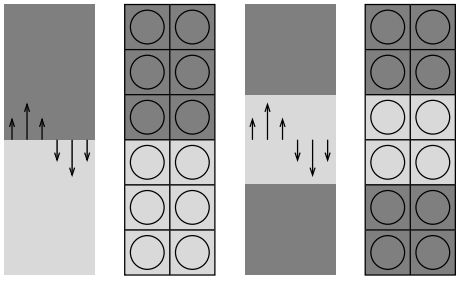

FIG. 1: Schematic representation of initial conditions and velocity field. Problem setup, from left to right: reaction enhancement in shear flow; reaction enhancement in cellular flow; quenching in shear flow; quenching in cellular flow. Dark tone corresponds to the cold fluid ($T = 0$), light – to the hot fluid ($T = 1$).

thick fronts. The computational domain extended a considerable distance upstream and downstream from the burning front so that boundary effects were negligible. In flame enhancement simulations the overall grid was remapped following the propagation of the front, thereby allowing for long integration periods — of the order of 1000 reaction times τ. We found that these long integrations were necessary in order to reproduce correctly the asymptotic behavior of the propagation speed in the case of strong advection.

As a measure of the reaction enhancement we use the bulk burning rate

$$v(t) = \frac{1}{L}\int_0^L \int_{-\infty}^{\infty} \frac{\partial T(x,y,t)}{\partial t}\, dydx = \frac{1}{\tau L}\int_0^L \int_{-\infty}^{\infty} R(T)\, dydx. \qquad (6)$$

The second equality in (6) can be justified by integration by parts. The bulk burning rate coincides with the front velocity in a case where the solution is a travelling wave, but provides a more flexible measure of combustion. Physically, $v(t)$ can be understood as the total amount of reacted material or the total heat production. In all simulations done for reaction enhancement, $v(t)$ approaches an asymptotic value (for cellular flows one should average in time to arrive at this value) and we denote this asymptotic value v.

We remark that in shear and cellular flows equation (1) admits travelling wave-type solutions, called pulsating fronts (see e.g. [9–11, 51, 52]). A rigorous stability theory for these solutions exists but is not complete (see [53] for a recent review). Except when quenching occurs, in our simulations we always observed convergence of the solution to such waves, so the bounds on v also provide bounds for the propagation speeds of pulsating fronts.

In the quenching studies, we measure the total amount of burned material per wavelength,

$$w(t) = \frac{1}{L}\int_0^L \int_{-\infty}^{\infty} T(x,y)\, dy\, dx, \qquad (7)$$

which can also be interpreted as the width of the non-perturbed horizontal band with temperature $T = 1$ surrounded by the fluid with $T = 0$. This quantity is related to the bulk burning rate per interface, $v(t) = \dot{w}(t)$. Depending on initial conditions and flow parameters, $w(t)$ either approaches an asymptotic value, e.g. $v(t) \to 0$, or increases with constant rate, that is $v(t) \to v$ (for cellular flow, in the time-averaged sense). In the first case we say that flame quenches; the main objective of quenching simulations is to determine under which conditions this happens.

III. SHEAR FLOW: REACTION ENHANCEMENT

We carried out simulations with the sinusoidal shear flow with amplitude flow U, and wavelength, L, given by Eq. (2). In this section we are interested only in reaction enhancement phenomena, and therefore for initial conditions we consider $T = 1$ in the semi-infinite domain $y < 0$, and $T = 0$ for $y > 0$. We carried out computations for both KPP and ignition type reactions, but did not find significant differences in the qualitative behavior. The numerical results presented in this section are obtained with KPP reaction term (4).

Of special interest is the dependence of the effective propagation rate v on the velocity amplitude, U, and wavelength, L, which defines the characteristic length scale of the flow (Fig. 2). For small amplitudes, $U \ll v_\circ$, our results are in agreement with the quadratic law $v \sim v_\circ + cU^2$, which goes back to Clavin and Williams [17] for turbulent flow and has been recently proved rigorously for shear flows in [29]. We did not study this regime in detail since our main interest is in the strong advection case.

For the amplitudes $U \gg v_\circ$ the results are in good agreement with the linear law $v = aU + b$, where the coefficients a and $b \le v_\circ$ depend on the geometry of the flow. In the situation where the scale of the flow is much larger than the reaction length scale, $L \gg \delta$, our data agrees with $v = U + v_\circ$. This law has been proposed in [6] for shear flows which vary slowly compared to the typical reaction length and rigorously proved in [20] under similar assumptions. For any fluid flow, the regime $L \gg \delta$ is closely related to the so-called geometrical optics combustion regime [42], the limit where reaction time

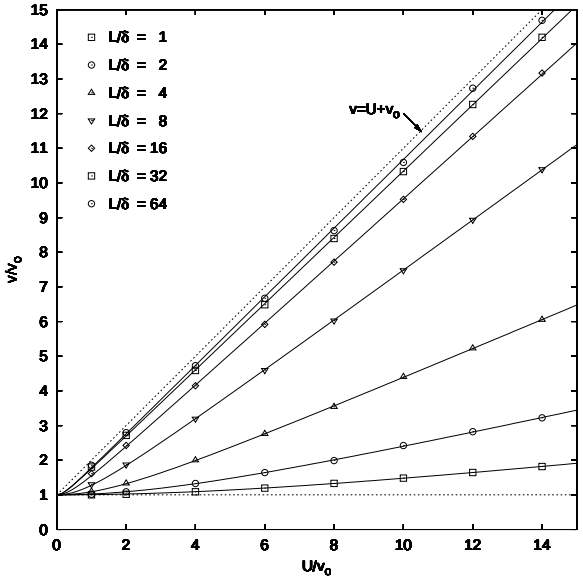

FIG. 2: Bulk burning rate (6) as a function of the shear flow amplitude for different shear wavelengths.

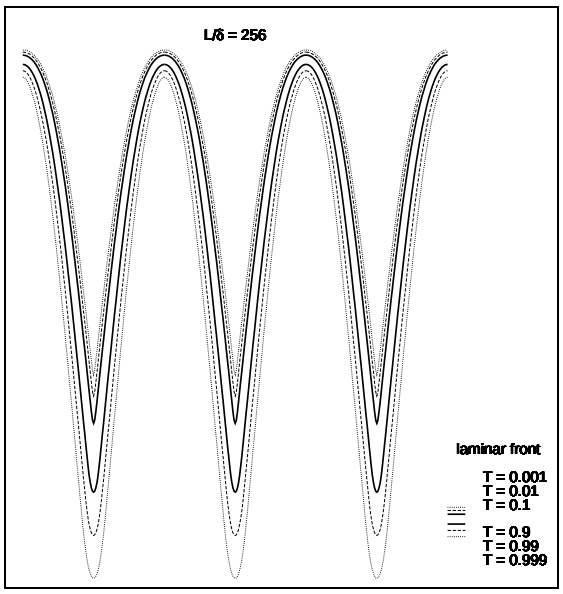

FIG. 3: Isotherms within the front in the geometrical optics limit. Here $L/\delta = 256$, and $U/v_\circ = 4$.

and length scales approach zero. In the framework of the equation (1) this corresponds to the limit $\kappa, \tau \to 0$ while κ/τ remains constant. Indeed, by rescaling equation (1) with a factor L/δ in space and time, we find that the bulk burning rate v for the original equation (1) is the same as for equation with modified diffusion and reaction (8)

$$T_t + \mathbf{u} \cdot \nabla T - \kappa \frac{\delta}{L} \Delta T = \frac{L}{\delta \tau} R(T). \tag{8}$$

As L grows, equation (8) approaches the geometrical optics limit.

Quite often, front propagation in the thin front and fast reaction limit is modelled by Hamilton-Jacobi type equations. One such model is the G-equation

$$G_t + \mathbf{u} \cdot \nabla G = v_\circ |\nabla G|, \tag{9}$$

where the front is defined by a constant level surface of the scalar G (see e.g. [38]). The G-equation describes propagation of the front according to Huygens principle; that is, the front (i) is transported by fluid flow, and (ii) propagates normal to itself with the speed $v_\circ$. The law $v = U + v_\circ$ can also be understood from the point of view of geometrical optics since it is easily derived from the G-equation. Recently Majda and Souganidis pointed out that the G-equation does not provide the geometrical optics limit of the reaction diffusion equation (8) in a precise sense [25, 37]. However the rigorous bounds derived for the true effective equation still give the same prediction for v in the case of shear flow [37].

In the situation where L becomes comparable to δ, the coefficient proportionality a between velocity amplitude and flame propagation rate is no longer equal to unity. The rigorous lower bound for v from [35] takes form $v \geq C_1 U \frac{1}{1+C_2 n}$, where $n = 2\pi\delta/L$. This bound is in good qualitative agreement with an argument proposed by Abel, Celani, Verni and Vulpiani [1] based on the effective diffusivity for the shear flow. It is well known that, if the problem is considered on sufficiently large time and length scales, the effect of the advection of passive diffusive scalar can often be modelled by effective diffusivity [7, 8]. The expression of effective diffusivity in a strong shear flow goes back to Taylor [48], $\kappa_{\text{eff}} = \kappa + \frac{1}{2}\left(\frac{U}{v_\circ m}\right)^2 \kappa$, where $m = 2\pi\delta/l$ and l is the typical length scale of the flow. In the presence of reaction, we take $l = \min(\delta, L)$, since the advection balances with reaction instead of diffusion if $L > \delta$. This leads to the qualitative prediction $v \sim U$ if $L \gg \delta$ and $v \sim UL/\delta$ if $L \lesssim \delta$. We obtained good although not perfect agreement with this prediction. This is not surprising given the heuristic derivation of the expression for the effective diffusivity and its possible dependence on more subtle geometric properties of the flow.

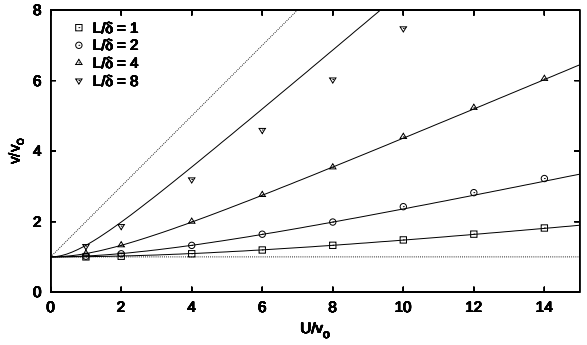

FIG. 4: Bulk burning rate in high wavenumber sinusoidal shear flow as function of shear amplitude (points), compared with isotherm elongation (solid lines) given by Eq. 10.

Additional understanding of linear dependence $v(U)$ can be gained from studying the relationship between the burning enhancement and the structure of the front, in particular level sets of the temperature. Assume that in the geometrical optics approximation the front is given by the function $y = f(x)$; then for the travelling wave obeying Huygens principle and propagating with speed v, we have

$$v = u(x) + v_\circ \sqrt{1 + (f')^2},$$

where $u(x)$ is profile of the shear, $u(x) = U \cos \frac{2\pi x}{L}$. In the case where u is a mean zero flow, this leads to the expression

$$v = \frac{v_\circ}{L} \int_0^L \sqrt{1 + (f')^2}\, dx. \tag{10}$$

Thus, we obtain a well-known fact that the speed of propagation is proportional to the area of the front which in

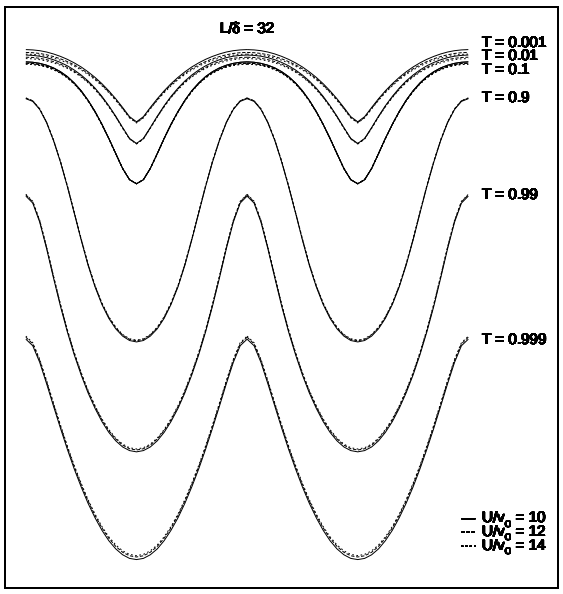

FIG. 5: Isotherms within the front for cases with $L/\delta = 32$ and $U/v_\circ = 10, 12, 14$. The individual curves have been rescaled by a factor of $(U/v_\circ)^{-1}$ in the y direction.

geometrical optics limit coincides with a level set of T (see Fig. 3 for a picture of level sets in a situation close to geometrical optics). It is interesting to test to what extent this relationship remains true in the situations where geometrical optics regime is no longer valid, for example when L is comparable to δ. We found that for large U, there is still good agreement between the elongation factor of the level sets of temperature and combustion enhancement (Fig. 4). Moreover, we found that for large U the temperature distribution across the front scales with the shear amplitude (see Fig. 5), providing another explanation of the linear dependence of the bulk burning rate on the amplitude of the flow. This scaling behavior can be understood in terms of the approximate self-similarity of equation (1) with respect to the change of variables $\tilde{y} = \frac{y/\delta}{U/v_\circ}$, $\tilde{x} = x/\delta$, $\tilde{t} = t/\tau$, which gives

$$\frac{\partial T}{\partial \tilde{t}} + \cos\left(\frac{2\pi x}{L}\right)\frac{\partial T}{\partial \tilde{y}} = \frac{\partial^2 T}{\partial \tilde{x}^2} + \left(\frac{v_\circ}{U}\right)^2 \frac{\partial^2 T}{\partial \tilde{y}^2} + R(T). \quad (11)$$

The only term which now depends on U is the one proportional to the second derivative in $\tilde{y}$, and it becomes negligible in the limit of large U. Indeed, equation (11) without this term is hypoelliptic, and so addition of the second derivative term does not constitute a singular perturbation. That leads to U-independent propagation rate $\tilde{v} \equiv \frac{v}{U} = \tilde{v}(L)$ and to linear proportionality $v \propto U$ for large $U/v_\circ$.

We conclude this section by a remark that understanding of the combustion enhancement in a shear flow appears to be useful in some situations where flows with different structure are involved. In particular, in the reactive Boussinesq system the flow consists of vortices moving along with the reaction front [54]. However in the frame moving with the front the effect of such vortical flow is similar to the shear. The prediction for the reaction enhancement in such system based on the results for the shear flows appears to be in agreement with numerically observed behavior [54].

IV. CELLULAR FLOW: REACTION ENHANCEMENT

Cellular flows have been studied by many authors (see e.g. [15, 22]), since similar fluid motions appear in many important applications; classical examples are the two-dimensional rolls of the Rayleigh-Bénard problem and Taylor vortices in Couette flow.

For cellular flow simulations, we use a velocity field given by Eq. (3). The flow is controlled by two parameters, velocity amplitude U and wavelength L. As in simulations of reaction enhancement by shear flow, we consider initial conditions with $T = 0$ in the upper half of the computational domain ($y < 0$), and $T = 1$ in the lower half ($y > 0$). Most of the results presented in this section were obtained with KPP reaction term (4); the influence of the reaction type on the reaction enhancement is discussed at the end of this section.

There are several regimes, which can be classified according to the relations between the characteristic scales present in the problem. There are three characteristic time scales: advection, $\tau_U = L/U$; reaction, $\tau_R = \tau$; and diffusion, $\tau_D = L^2/\kappa$. In this paper, we mostly studied two regimes: $\tau_U \ll \tau_R \ll \tau_D$ and $\tau_R \ll \tau_U \ll \tau_D$. The first is the regime of strong advection; in the second regime advection can be very strong as well, but is compensated by large cell size L, so that the reactive time scale becomes the fastest in the problem. If $\tau_D \ll \tau_R$, or equivalently, $L \ll \delta$, we have diffusive or small cell regime. The remaining regime corresponds to $\tau_R \ll \tau_D \ll \tau_U$, and therefore $U \ll v_\circ$. Hence we have slow advection; this situation is of less interest to us since $v \le U + v_\circ$ under very general conditions [19], so the effect of the advection on the propagation speed is minor.

In the regime $\tau_R \ll \tau_U \ll \tau_D$ our simulations show good agreement with geometrical optics models. In Figure 7 we show a typical picture of flame in the regime close to geometrical optics. The G-equation, (9), which is closely related to geometrical optics regime, is invariant under simultaneous rescaling of time and space by the same factor. This suggests that for flames approaching the geometrical optics limit, one should observe this similarity, and indeed we do as shown in Fig. 7. The earliest prediction of the front propagation speed in a cellular flow for large U within the geometrical optics framework appears to be due to Shy, Ronney, Buckley and Yakhot [47]. Using heuristic reasoning, they proposed that $v \sim U/\log(U/v_\circ)$ if one considers front advancing according to Huygens principle. The same law

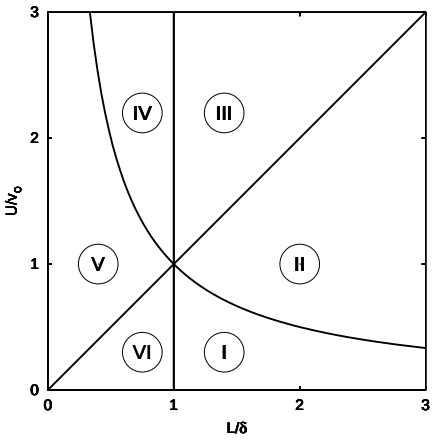

FIG. 6: Burning regimes in cellular flow: (I) $\tau_R < \tau_D < \tau_U$ — slow advection geometrical optics; (II) $\tau_R < \tau_U < \tau_D$ — fast advection geometrical optics; (III) $\tau_U < \tau_R < \tau_D$ — fast advection with radial burning within cells; (IV) $\tau_U < \tau_D < \tau_R$ — fast advection with uniform burning within cells; (V) $\tau_D < \tau_U < \tau_R$ — limited advection in small cells; (VI) $\tau_D < \tau_R < \tau_U$ — slow advection in small cells.

is proposed in [2] based on more detailed analysis. To illustrate the origin of this law, let us sketch an argument providing the lower bound for v. Let us look at the propagation of the flame tip along the path ABCDE on the Fig. 8. Assuming that at every point of ABCDE the flame velocity is given by $u(x,y)+v_\circ$, and integrating in time, we obtain a lower bound

$$\frac{v}{v_\circ} \geq \frac{\pi}{4} \frac{\sqrt{\left(\frac{U}{v_\circ}\right)^2 - 1}}{\log\left(\frac{U}{v_\circ} + \sqrt{\left(\frac{U}{v_\circ}\right)^2 - 1}\right)}. \qquad (12)$$

This lower bound, when doubled, gives a very good fit to our numerical data and is represented by a solid line in Fig. 9. As one can see in Fig. 7, the tip of the flame follows the path close to ABCDE, but avoiding corners; this may account as a factor for the difference in speed compared with the lower bound. Our results in the geometrical optics regime agree with results of [2]; however we stress that our simulation was carried out for the reaction-diffusion equation (1) using the same numerical scheme in all regimes, while [2] uses a different model in geometrical optics limit. We remark that in [1, 2] the possibility of the regime, where $\tau_R \ll \tau_U$ and v behaves as $U^{3/4}$, was proposed. We could not definitively confirm existence of such a regime due to the closeness of $(U/v_\circ)^{3/4}$ and $(U/v_\circ)/\log(U/v_\circ)$ curves in the range of tested parameters (Fig. 9).

It should be emphasized that the geometrical optics regime requires not only the thin front assumption, $L \gg \delta$, but also fast reaction in comparison with advection, $\tau_R \ll \tau_U$; in other words, velocity must be limited by $U \ll (L/\delta)\, v_\circ$. When this restriction is broken we observe

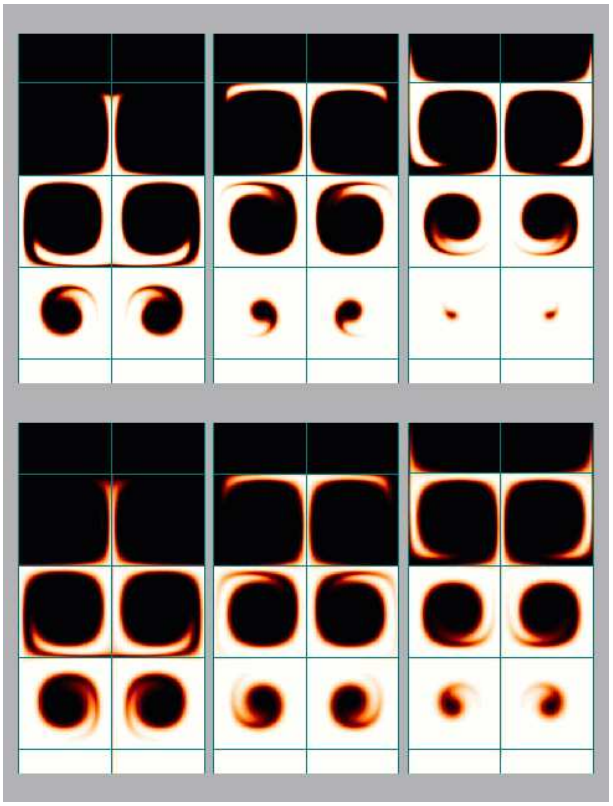

FIG. 7: Flame in cellular flow with amplitude $U/v_\circ = 20$ and period $L/\delta = 1024$ (upper row) and $L/\delta = 512$ (lower row). Snapshots for the first case were taken with time interval $24\,\delta/v_\circ$ and for the second - with time interval $12\,\delta/v_\circ$.

significant decrease in flame propagation speed compared to the geometrical optics prediction (Fig. 9). Figure 10 further illustrates this point, showing that on a logarithmic scale, there is a marked change in the slope of $(v/v_\circ)$ as a function of U as τ_R/τ_U increases. When τ_U exceeds τ_R, we observe power-law, $v \sim U^{1/4}$, as proposed by Audoly, Berestycki and Pomeau [6], and confirmed in [2] in a narrower range of parameters. The measurement of the slope 1/4 was sufficiently precise to distinguish it from the $v \sim U^{1/5}$ behavior, a lower bound rigorously proved in [35]. The observed $v \sim U^{1/4}$ scaling extends to the limit of cell sizes small in comparison with the laminar thickness, $L \ll \delta$. We remark that the laminar front thickness for the KPP reaction is of the order of $16\,\delta$ which is large compared to smallest cell size $L/2 = 4\,\delta$ shown in Fig. 10; limited data available for $L/\delta = 4, 2$ (shown in Fig. 11) also confirms the $v \sim U^{1/4}$ scaling. In the very small cell regime, the $v \sim U^{1/4}$ scaling was rigorously proven in [29] using homogenization approach.

We also studied the dependence of v on the cell size while $U/v_\circ$ is fixed. Figure 12 shows changes in the structure of the flame with the increase of the cell size — from a more diffusive front to a front approaching geometrical optics behavior. The flame propagation speed, normalized by $(U/v_\circ)^{1/4}$ factor, is presented in Fig. 11. As L/δ

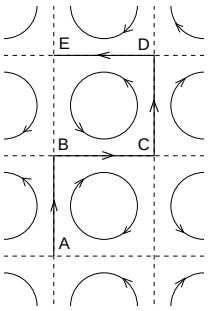

FIG. 8: Approximate path of the tip of the flame

increases, we see the transition from the $\tau_U \ll \tau_R$ regime, to the geometrical optics, where flame propagation speed is independent of cell size. For $\tau_U \ll \tau_R$ the data collapse to a single curve, suggesting the power scaling with L/δ, with power changing from 1/4 for small L/δ to 3/4 for large L/δ. The resulting scaling can be summarized as,

$$v/v_\circ \sim (U/v_\circ) / \log(U/v_\circ), \quad \tau_R \ll \tau_U \ll \tau_D, \quad (13)$$

$$v/v_\circ \sim (U/v_\circ)^{1/4} (L/\delta)^{3/4}, \quad \tau_U \ll \tau_R \ll \tau_D. \quad (14)$$

$$v/v_\circ \sim (U/v_\circ)^{1/4} (L/\delta)^{1/4}, \quad \tau_U \ll \tau_D \ll \tau_R, \quad (15)$$

To explain observed the flame propagation speed, let us consider a model based on the effective diffusivity, proposed by Audoly, Berestycki and Pomeau [6]. When velocity is high, $\tau_U \ll \tau_R$, the sharp temperature gradients appear in the narrow boundary layer at cell borders (Fig. 13). The thickness of the boundary layer, h, is determined by the balance of diffusion and advection, $\kappa/h^2 = U/L$, and is much smaller than δ,

$$h \sim \sqrt{\kappa L/U}. \quad (16)$$

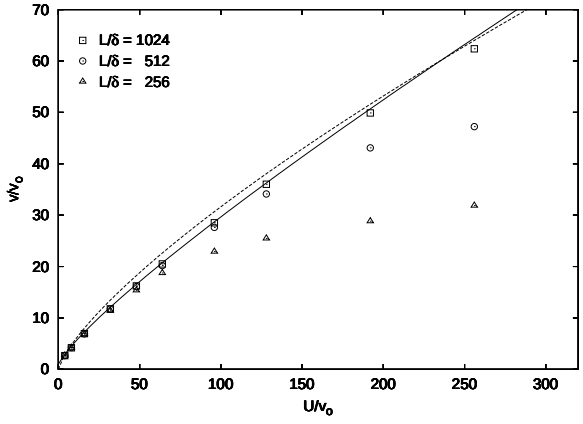

FIG. 9: Flame propagation velocity in thin flame regime as function of the cellular flow amplitude. Solid line is doubled Eq.(12), dashed line is $v/v_\circ = (U/v_\circ)^{3/4}$.

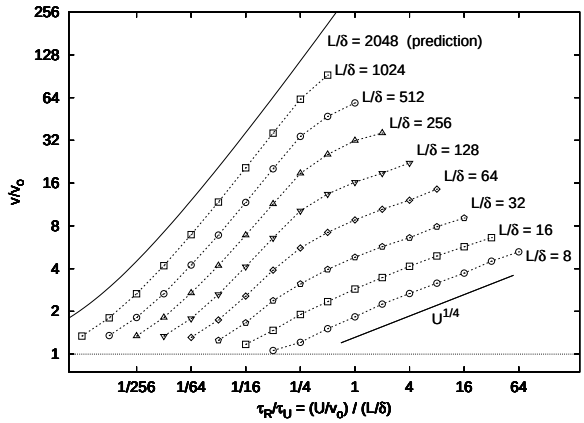

FIG. 10: Flame propagation velocity as function of the ratio of laminar burning time to the vortex turnover time. The $L/\delta = 2048$ prediction is based on doubled Eq. (12) for geometrical optics.

(This argument is a concise, naive version of the considerations appearing in the derivation of the effective diffusivity in cellular flow, [16, 45, 46, 56].)

A discrete diffusion equation modelling the original equation (1) has been suggested in [1, 2]:

$$\frac{\partial \theta_n}{\partial t} = \frac{\kappa_{\text{eff}}}{L^2} [\theta_{n-1} - 2\theta_n + \theta_{n+1}] + \frac{1}{\tau} R(\theta_n). \quad (17)$$

Here θ_n is the average temperature in the n-th cell; and κ_{eff} is effective diffusivity

$$\kappa_{\text{eff}} = \kappa\, L/h. \quad (18)$$

This leads to the propagation rate,

$$v = \sqrt{\kappa_{\text{eff}}/\tau} \sim v_\circ \sqrt{L/h},$$

and, taking into account Eq. (16), to the scaling (15). We found that the prediction for speed given by (17) agrees with numerical simulations only if $L \lesssim \delta$.

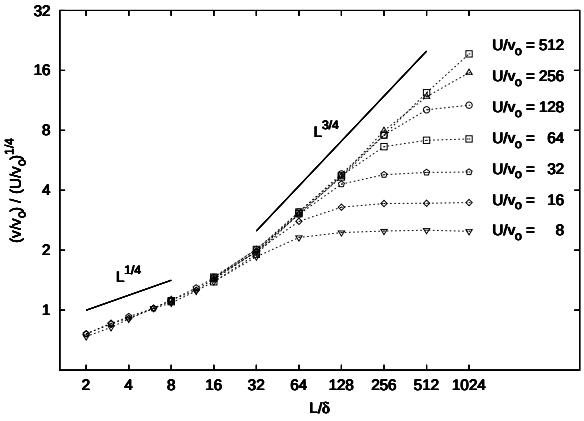

FIG. 11: Dependence of the flame propagation velocity on the size of the vortex.

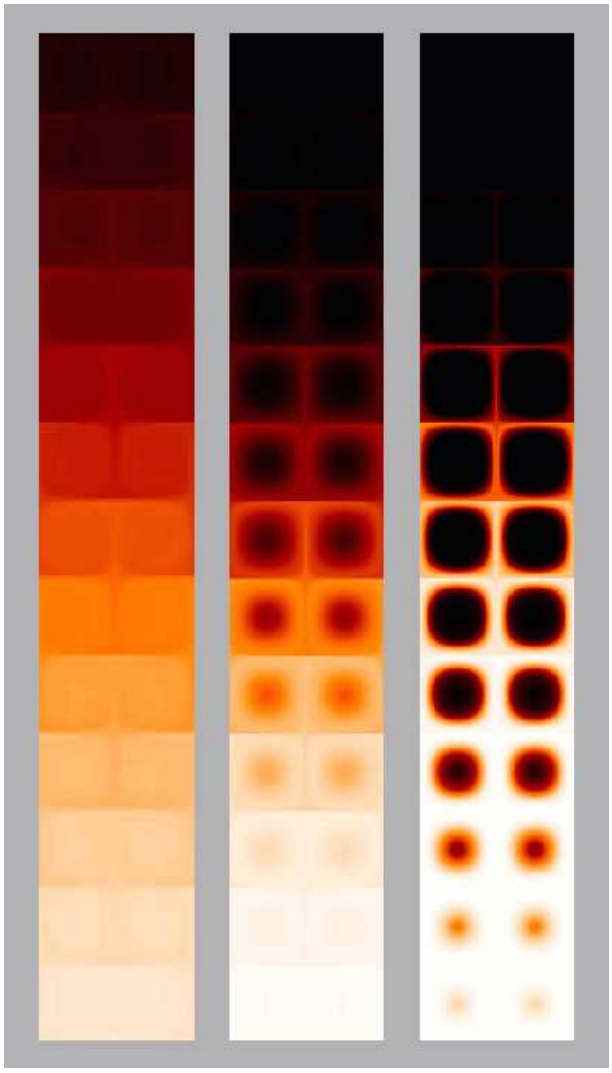

FIG. 12: Flame in a cellular flow with amplitude $U/v_\circ = 100$ and period $L/\delta = 16, 64, 256$ (left to right)

For large cell sizes, $L \gg \delta$, the diffusive model (17) no longer accounts fully for the flame propagation process. The main objection to the model is that (17) assumes temperature is uniform inside the cell, and the reaction term can be estimated at the average cell temperature. However the numerically observed behavior demonstrates at first sharp temperature gradients at the border of the cell, later evolving into flame propagation inside of the cell roughly at the laminar flame speed (see Fig. 13 for the structure of the front inside cells). Indeed, the cellular flow has no efficient mechanism for mixing between the streamlines, and the diffusion time scale in that direction is of the order L^2/κ (practically not enhanced) [41]. Therefore the combustion process inside the cell takes time of the order of $L/v_\circ$, rather then $\delta/v_\circ$ (which corresponds to substituting the average temperature into the reaction term).

Here, we will modify the effective diffusivity model (17) to account for slower burning inside large cells. As in the case of small cells, the flame propagation from one cell to another is enhanced because of the high temperature gradient in the boundary layer with width given by expression (16). The heat coming to the cell through the cell boundary is distributed on the scale of δ (as opposed to L, in the case of small L). We further notice that due to the fast advection, the temperature is essentially equal along the streamlines inside the cell (see Fig. 12), which allows the flame to propagate directly from one boundary layer to another (Fig. 13). That allows us to write the discrete diffusion equation similar to (17), but replacing averaging in the cell by the averaging in the strip of width δ along the cell border (δ-layer),

$$\frac{\partial \theta_n}{\partial t} = \frac{\kappa_{\text{eff}}}{\delta^2}\left[\theta_{n-1} - 2\theta_n + \theta_{n+1}\right] + \frac{1}{\tau}R(\theta_n). \qquad (19)$$

Here θ_n is the average of the temperature in the δ-layer of the n-th cell; and κ_{eff} is effective diffusivity,

$$\kappa_{\text{eff}} = \kappa\,\delta/h. \qquad (20)$$

The temperature in a laminar front varies on the scale δ, and so estimating reaction in a δ-layer by $R(\theta_n)$ is justified. Equation (19) does not take into account the heat flux from the δ-layer to the bulk of the cell. However, since $h \ll \delta$, this heat flux does not enter the main balance. In other words, the front described by (19) propagates entirely in the δ-layers, with the rate $v_\delta = \sqrt{\kappa_{\text{eff}}/\tau} \sim v_\circ\sqrt{\delta/h}$. Substituting h from Eq. (16) we obtain,

$$v_\delta \sim v_\circ\,(U/v_\circ)^{1/4}(L/\delta)^{-1/4}. \qquad (21)$$

The time needed to ignite a new cell, e.g. to warm up a layer of the size of the order δ in that cell, is equal to $\tau_\delta = \delta/v_\delta$. Once the width of a warmed up layer reaches size of the order of δ, reaction becomes capable of sustaining the temperature. Further propagation of the flame corresponds to the basically laminar front movement inside the cell, and takes time $\tau_{\text{cell}} \sim L/v_\circ$.

The total bulk burning rate v is of the order of $v_\circ$ times the number of burning cells, which can be estimated as the ratio of the cell burning time, $\tau_{\text{cell}} \sim L/v_\circ$, to the time needed to ignite a cell, $\tau_\delta = \delta/v_\delta$. Therefore the bulk burning rate is obtained by multiplying the number of burning cells with $v_\circ$, or essentially by normalizing v_δ with a factor of L/δ,

$$v \sim v_\circ\frac{\tau_{\text{cell}}}{\tau_\delta} \sim \frac{L}{\delta}\,v_\delta \sim v_\circ\,(U/v_\circ)^{1/4}(L/\delta)^{3/4},$$

which agrees with numerically observed scaling (14).

Finally, we would like to mention the effect of the reaction rate. Similar to the shear flow, we found that the reaction type does not influence asymptotic scaling laws like (15) or (14), although there is certainly a difference in the constant factors. However, in cellular flows there is an interesting phenomenon which is present for ignition-type but not KPP reactions. The dependence $v(U)$ is

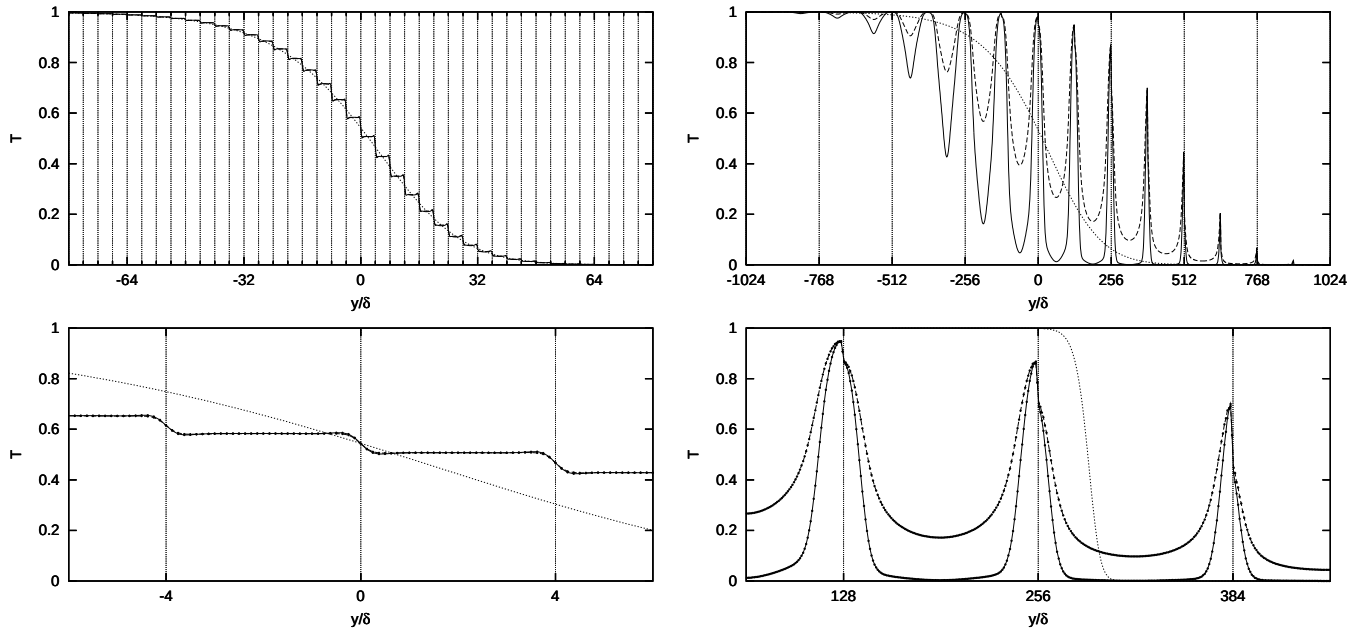

FIG. 13: Temperature profile at the middle of the cell (solid) and temperature averaged in x-direction (dashed) for $L/\delta = 8, U/v_\circ = 64$ (left) and for $L/\delta = 256, U/v_\circ = 128$ (right). Bottom plots are blow up versions of top plots. Dotted line in the top plots represents laminar front stretched by factor $v/v_\circ$ in y-direction, while in the bottom plots it represents non-modified laminar front.

always monotone increasing in the KPP case, but it may exhibit a temporary reversal for ignition-type reactions (Fig. 14). This effect has been discovered by Kagan and Sivashinsky [30] and further studied in [31]. We found that this phenomenon is more pronounced when the reaction threshold $T_\circ$ is closer to unity, in agreement with the arguments of [31].

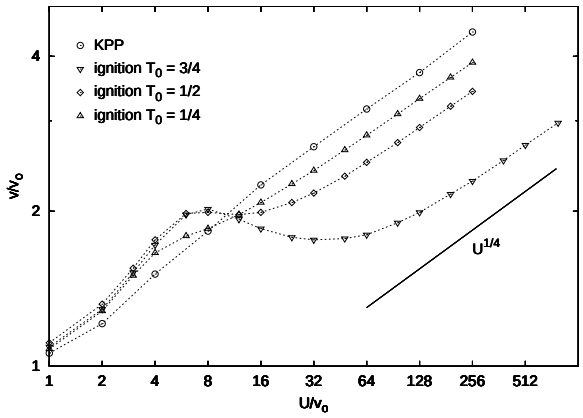

FIG. 14: Flame propagation velocity for different reactions ($L/\delta = 8$).

V. QUENCHING

In this section we address another effect that advection can have on the combustion process — quenching. We say that reaction is quenched if the average temperature goes to zero uniformly with time. Quenching occurs in the systems with ignition type reaction when, due to diffusion and advection, temperature drops below the ignition threshold everywhere and the integrated reaction rate becomes identically zero.

If the size of the region is small enough quenching can be caused by diffusion alone, e.g. without advection, as shown by Kanel [32]. Kanel considered the one-dimensional reaction-diffusion equation $T_t - \kappa T_{xx} = \tau^{-1} R(T)$. He found that there exist two critical sizes $W_\circ \le W_\circ^*$ such that if the initial size of the hot region (where $T = 1$) is smaller than $W_\circ$, reaction quenches, while if the initial size of the hot region is greater than $W_\circ^*$, two fronts form and propagate in opposite directions. Two different critical sizes are likely an artifact of the proof; in our simulations, we always found $W_\circ = W_\circ^* \sim \delta$ and will refer to the single critical size $W_\circ$. In two and three dimensions, the presence of advection may lead to stretching of the initial hot spot, thus making diffusion more efficient at cooling, and consequently, at quenching.

In our numerical simulations we study quenching under the influence of advection, in particular in shear and cellular flows. As in previous sections, the prescribed flow velocities are defined by Eq. (2) for shear flow and by Eq. (3) for cellular flow. For all simulations we used

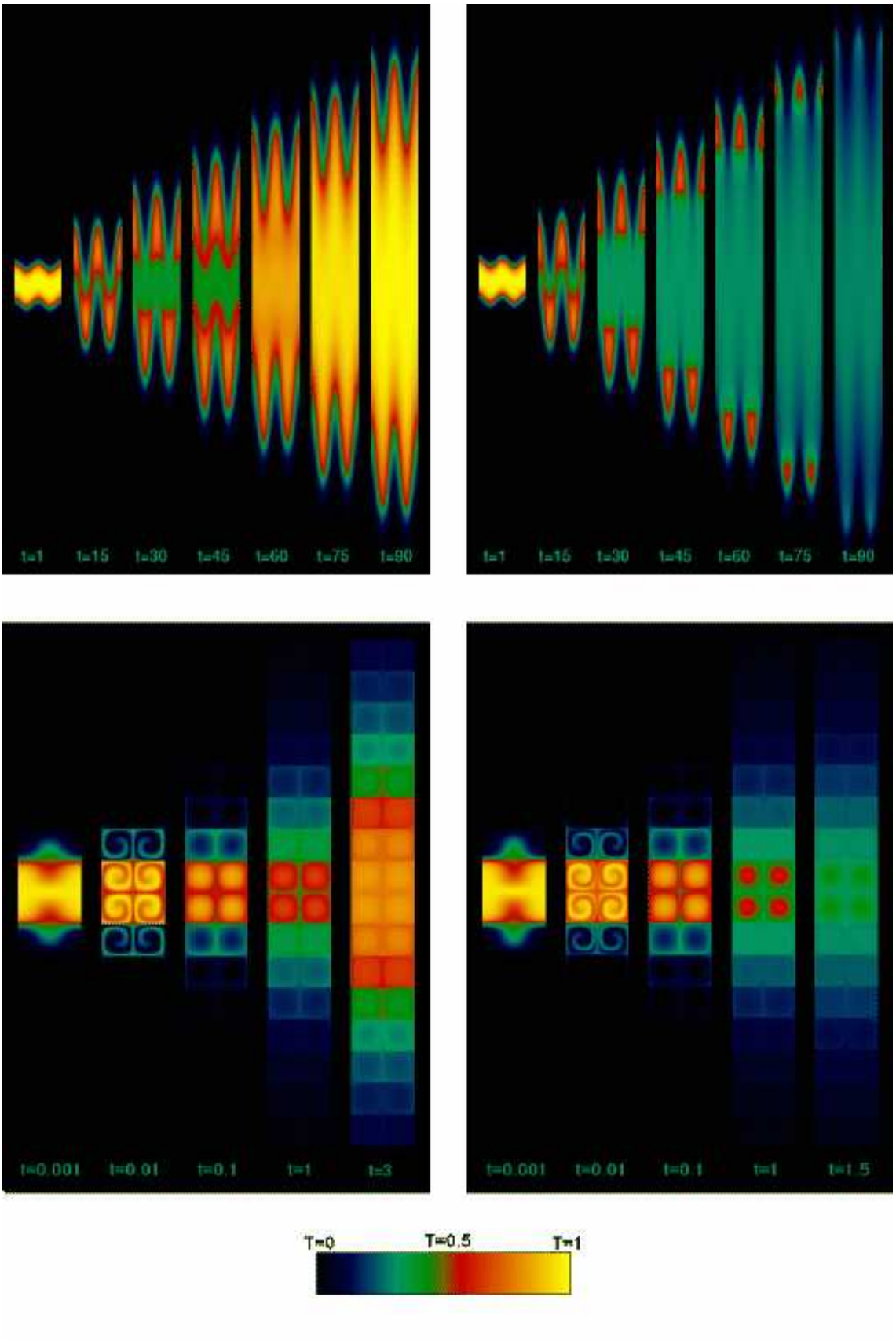

FIG. 15: Sequence of snapshot of temperature distribution in the shear flow with $L/\delta = 4$ (top) and in the cellular flow with $L/\delta = 4$ (bottom). Initial condition was a hot band of the width $W/\delta = 6$ and $W/\delta = 4$ for shear and cellular flow simulations respectively. Velocities amplitudes are below critical on the left and above critical on the right (shear: $U/v_\circ = 13$ and $U/v_\circ = 14$; cellular: $U/v_\circ = 600$ and $U/v_\circ = 800$). The time is given in units of τ.

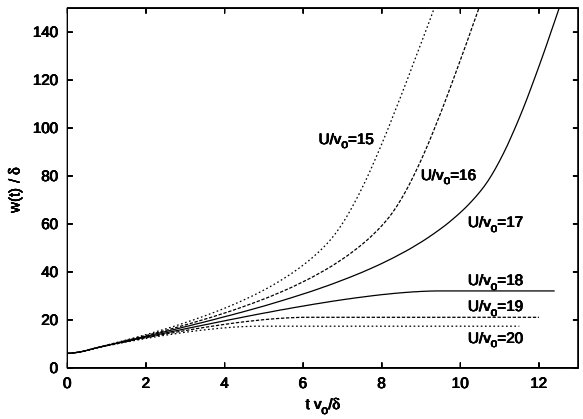

FIG. 16: Temperature integrated over area $0 < x < L$, $-\infty < y < \infty$ per wavelength L for different values of shear amplitude U, measured for $L/\delta = 6$ and $W/\delta = 6$.

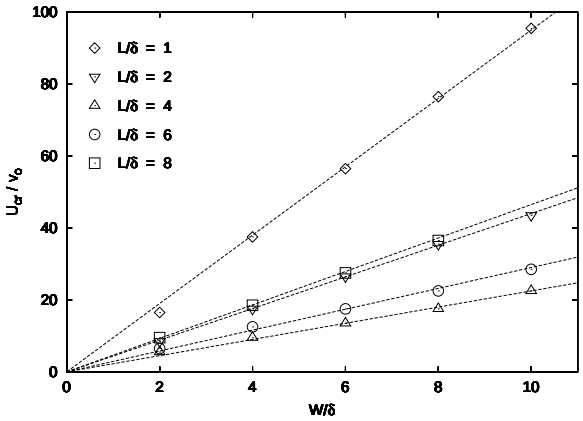

FIG. 17: The critical amplitude of shear flows with different wavelengths as function of initial width of hot band.

the ignition-type reaction (5) with threshold $T_\circ = 1/2$, since quenching cannot occur for the KPP-type source term [43, 44]. As the initial conditions we use a horizontal band of width W with temperature above critical ($T = 1$) within the band and with temperature below critical ($T = 0$) outside the band.

The typical evolution of the system described above is shown in Fig. 15. We found that the temperature distribution in both for shear and cellular flows evolves according to one of the two possible scenarios, depending on the amplitude of the advection velocity. For lower advection velocities, after an initial transient period, the system develops solution characterized by a wide, steadily growing burned region between two wrinkled fronts propagating in opposite directions. These fronts are exactly as described in the preceding sections with regard to structure, speed, and dependence on the flow properties U and L. For higher advection velocities, the temperature eventually drops below $T_\circ$ everywhere, after which no burning occurs. We denote by $U_{\rm cr}$ the value of advection velocity which triggers the system between these two scenarios (further we refer to them as burning and quenching), and establish the relation between $U_{\rm cr}$ and the initial conditions and structure of the flow.

We measure the critical value of velocity amplitude $U_{\rm cr}(L, W)$ using the following procedure. For each combination of the initial hot band size W and velocity period L, we execute a number of simulations for different velocity amplitudes U. For each simulation we measured the total amount of burned material per period $w(t)$, defined by Eq. (7), as a function of time (shown in Fig. 16). The burning systems (with higher velocities, where two front are formed) are characterized in Fig. 16 by constant, non-zero slopes, corresponding to constant reaction rate. These rates are independent of initial conditions, and are equal to double the burning rate $v(U, L)$, since there are two fronts. The quenched systems are characterized by evolving to constant $w(t)$. Both formation of steady fronts and quenched solutions requires some transition time.

The summary of results for a sinusoidal shear flow is given in Fig. 17 and Fig. 18. We found that $U_{\rm cr}$ scales linearly with W (see Fig. 17),

$$U_{\rm cr} = \alpha \frac{W}{\tau}, \tag{22}$$

as predicted in [20], with the coefficient α strongly dependent on the wavelength of the advection velocity (Fig. 18). Shear flow is most effective at quenching in the intermediate range of wavelengths, namely when L is of the order of a few reaction lengths δ. The quenching mechanism for small and for large L is different; one has to distinguish between the ability of the flow to stretch the front over the larger scales and to make the initial hot band uniformly thin.

For small L, the rapid spatial variation of the flow velocity is well approximated by effective diffusion. The effective diffusivity for strong shear flow scales as $\kappa_{\rm eff} \sim U^2 l^2/\kappa$, where $l = \min(\delta, L)$. The characteristic length

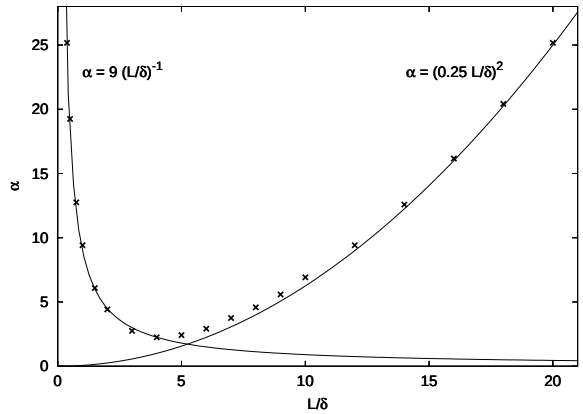

FIG. 18: Dependence of the factor α in Eq. (22) on the wavelength of shear flow L. Measurements were taken at $W/\delta = 6$

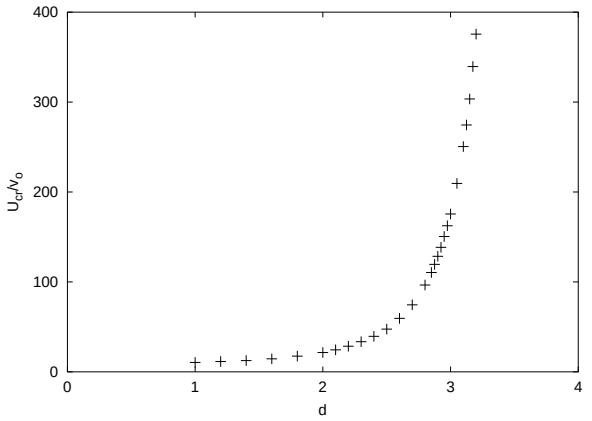

FIG. 19: Growth in the value of $U_{\rm cr}$ for a fixed W as the size of flat plateau increases.

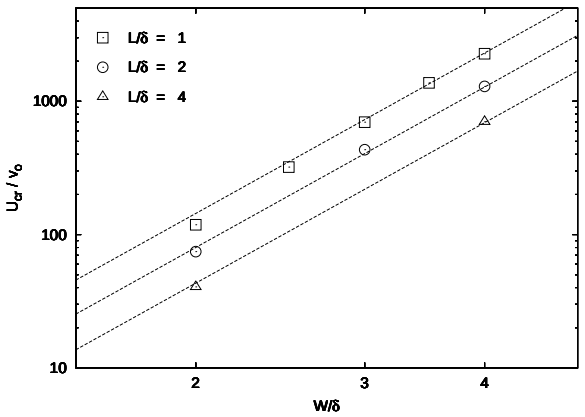

FIG. 20: The value of $U_{\rm cr}$ for cellular flows with different periods.

scale for reaction with this renormalized diffusion behaves as $l_{\rm eff} \sim \sqrt{\kappa_{\rm eff}\tau}$ and scales linearly with U. Then $l_{\rm eff} \sim W$ gives $U_{\rm cr} \sim \frac{\delta}{L} W\tau^{-1}$ for small L. We remark that in the limit of small L, the effective diffusivity argument can be justified by a rigorous homogenization procedure [29].

For large L, the nature of quenching is related to the appearance of the (almost) constant regions in the velocity profile. We observe the behavior $U_{\rm cr} \sim L^2$ for large L, which can be explained in the following way. In order for quenching to occur, the shear flow should stretch the initial hot region thinner than Kanel's critical length (of the order δ) in time less than the reaction time τ, so that reaction does not have time to compensate cooling by advection. The stretching is least efficient near the tip of the velocity profile. At the tip of a sinusoidal profile, the difference between flow velocities at two points separated by a distance δ is $U(\delta/L)^2$. Therefore we obtain a sufficient condition for quenching $U_{\rm cr}\left(\frac{\delta}{L}\right)^2\tau \sim W$, which leads to

$$U_{\rm cr} \sim \tau^{-1} W \left(\frac{L}{\delta}\right)^2.$$

We also examined a degenerate case of shear flows with a plateau in the velocity profile. For such flows it has been shown in [20] that quenching does not happen as soon as the size of plateau is larger than certain critical size of the order δ and the size of initial bandwidth W exceeds $W_\circ$. As expected, we found that $U_{\rm cr}$ diverged to infinity as the size of the plateau approached a critical value (Fig. 19), in agreement with results of [20]. This phenomenon can be understood in terms of reaction and diffusion alone: in the region where the profile of the velocity is flat, there is no stretching of the initial hot band. If the size of the hot band is roughly larger than Kanel's critical size $W_\circ$, then reaction can compete with diffusion, there will be no quenching, and eventually propagating fronts will form.

Quenching in cellular flow requires significantly higher advection amplitudes. For relatively small cell sizes $L \lesssim \delta$ where quenching is possible, we find that the critical velocity $U_{\rm cr}$ satisfies $U_{\rm cr} \sim W^4$ (see Figure 20). Notice that this correlates with the dependence $v \sim U^{1/4}$ for the speed of advection-enhanced flame. This correlation is not coincidental, and can be explained as follows. The speed up law indicates that the size of the region where reaction happens in a stabilized combustion regime scales as $(U/v_0)^{1/4}(L/\delta)^{1/4}\delta$ for large U. If the width of the initial band of hot material is of the order smaller than $(U/v_\circ)^{1/4}(L/\delta)^{1/4}\delta$, advection carries away the energy of the hot material over the larger region faster than reaction is able to compensate the falling temperature. This leads to quenching.

We remark that quenching is impossible if the cell size is sufficiently large, $L \gtrsim \delta$, and $W \gtrsim \delta$. The reason is similar to the flat plateau effect in the shear flow. Fluid advection does not provide mixing inside cells in the direction perpendicular to the streamlines, and thus if the cell is large enough reaction can sustain itself against diffusion. This result has been proved in [21].

VI. CONCLUSIONS

We carried DNS calculations of an advected scalar which reacts according to a nonlinear reaction law. We studied combustion enhancement and quenching phenomena in two typical classes of flows, shear and cellular. In a shear flow, we find linear dependence $v = aU + b$ of the combustion speed v on the amplitude of the flow U in the strong flow regime. The factor a depends on the relationship between the period of the flow L and typical reaction length scale δ, is equal to 1 if $L \gg \delta$ and tends to zero if $L/\delta \to 0$. The observed behavior is in agreement with recent rigorous [19] and numerical [1] results. In a cellular flow we studied primarily two regimes characterized by the relationships $\tau_D < \tau_U < \tau_R$ and $\tau_D < \tau_R < \tau_U$ between diffusion, reaction and advection time scales. We found that combustion speed in the first regime is

close to predictions of models based on geometrical optics limit, $v \sim U/\log(U/v_\circ)$. In the second regime where large U dominates, we found $v \sim v_\circ(U/v_\circ)^{1/4}(L/\delta)^{3/4}$. This agrees with the prediction of the effective diffusion model [1, 2, 6] in terms of the power of U but has different dependence the cell size L. We proposed an explanation of the observed behavior with a modified effective diffusion model where enhanced diffusivity is concentrated in the boundary layers.

As opposed to combustion enhancement, quenching may happen if the reaction term is of ignition type and initial temperature is higher than critical in a finite region. If the shear flow velocity profile does not have a plateau of sufficiently large size, or the size of the cells in cellular flow is not too large, then for any initial hot band size W there exists $U_{\rm cr}(W)$ such that for $U > U_{\rm cr}$ quenching takes place. If $U < U_{\rm cr}$, two fronts form and propagate with the speed of the developed advection-enhanced front. In the case of shear flow, $U_{\rm cr}$ depends linearly on W with a factor $\alpha(L)/\tau$. Quenching is most efficient for the flows with L on the order of a few typical reaction lengths δ. For the cellular flows, $U_{\rm cr}$ scales as W^4. The results are in good agreement with theoretical arguments.

VII. ACKNOWLEDGEMENTS

This research is supported in part by the ASCI Flash center at the University of Chicago under DOE contract B341495. PC was supported partially by NSF DMS-0202531. AK has been supported by NSF grants DMS-0102554 and DMS-0129470 and Alfred P. Sloan Fellowship. LR was supported partially by NSF grant DMS-0203537 and by an Alfred P. Sloan Research Fellowship.

[1] M. Abel, A. Celani, D. Vergni and A. Vulpiani, *Front propagation in laminar flows,* Physical Review E, **64** 6307 (2001).

[2] M. Abel, M. Cencini, D. Vergni and A. Vulpiani, *Front speed enhancement in cellular flows,* Chaos **12**, p. 481.

[3] R.C. Aldredge, in *Modelling Combustion in Science*, ed. by J. Buchmaster and T. Takeda, p. 23, (Springer-Verlag 1995).

[4] M.S. Anand and S.B. Pope, *Calculations of premixed turbulent flames by PDF methods,* Combust. Flame **67**, 127 (1987).

[5] D.G. Aronson and H.F. Weinberger, *Multidimensional diffusion arising in population genetics,* Adv. in Math., **30**, 1978, 33-76.

[6] B. Audoly, H. Berestycki and Y. Pomeau, *Réaction diffusion en écoulement stationnaire rapide,* C. R. Acad. Sci. Paris **328**, Série IIb, p. 255 (2000).

[7] M. Avellaneda and A. Majda, *Stieltjes integral representation and effective diffusivity bounds for turbulent transport,* Phys. Rev. Lett. **62**, p. 753 (1989).

[8] M. Avellaneda and M. Vergassola, *Stieltjes integral representation of effective diffusivities in time dependent flows,* Phys. Rev. E **52**, p. 3249 (1995).

[9] H. Berestycki, *The influence of advection on the propagation of fronts in the reaction-diffusion equations,* proceedings NATO ASI conf. Cargese, H. Berestycki & Y. Pomeau, eds. Kluwer (to appear).

[10] H. Berestycki and F. Hamel, *Front propagation in periodic excitable media,* Comm. Pure Appl. Math. 55 (2002), no. 8, 949–1032

[11] H. Berestycki, B. Larrouturou and P.L. Lions, *Multidimensional travelling wave solutions of a flame propagation model,* Arch. Rational Mech. Anal., **111**, 1990, 33-49.

[12] R. Borghi, in *Recent Advances in Aerospace Science*, ed. by C. Bruno and C. Casci, p. 117 (1985).

[13] D. Bradley, in *Twenty-Fourth Symposium (International) on Combustion*, The Combustion Institute, p. 247 (1992).

[14] K.N.C. Bray and N. Peters, in *Turbulent Reacting Flows*, ed. by P.A. Libby and F.A. Williams, p. 63 (Academic Press 1994).

[15] S. Chandrasekhar, *Hydrodynamic and Hydromagnetic Stability,* Dover Publications, Inc. 1990.

[16] Childress, S. *Alpha-effect in flux ropes and sheets,* Phys Earth Planet Inter. **20**, 172–180 (1979)

[17] P. Clavin and F.A. Williams, J. Fluid Mech. **90**, 589 (1979).

[18] P. Clavin and F.A. Williams, *Effects of molecular-diffusion and of thermal-expansion on the structure and dynamics of premixed flames in turbulent flows of large scale and low intensity,* J. Fluid Mech, **116**, 251 (1982).

[19] P. Constantin, A. Kiselev, A. Oberman and L. Ryzhik, *Bulk burning rate in passive-reactive diffusion,* Arch. Rat. Mech. Anal. **154** (2000), 53–91.

[20] P. Constantin, A. Kiselev and L. Ryzhik, *Quenching of flames by fluid advection*, Commun. Pure Appl. Math. **54**, p. 1320 (2001).

[21] P. Constantin, A. Kiselev and L. Ryzhik, *in preparation.*

[22] P.G. Drazin and W.H. Reid, *Hydrodynamic Stability,* Cambridge University Press, Cambridge, 1981

[23] T. Echekki and J.H. Chen, *Unsteady strain rate and curvature effects in turbulent premixed methane-air flames,* Combust. Flame **106**, 184 (1996).

[24] T. Echekki and J.H. Chen, *Analysis of the contribution of curvature to premixed flame propagation,* Combust. Flame **118**, 308 (1999).

[25] P. Embid, A. Majda and P. Souganidis, *Comparison of turbulent flame speeds from complete averaging and the G-equation,* Phys. Fluids, **7**, 1995, 2052-2060.

[26] P.C. Fife, *Mathematical Aspects of Reacting and Diffusing Systems,* Lect. Notes Biomath, **28**, Springer-Verlag, New York, 1979.

[27] R. Fisher, *The wave of advance of advantageous genes,* Ann. Eugenics, **7**, 1937, 355-369.

[28] A. Hanna, A. Saul and K. Showalter, *Detailed studies of propagating fronts in the iodate oxidation of arsenous acid,* J. Am. Chem. Soc. **104**, 3838 (1982).

[29] S. Heinze, G. Papanicolau and A. Stevens, *Variational principles for propagation speeds in inhomogeneous media,* SIAM J. Appl. Math. **62** no. 1, 129 (2001).

[30] L. Kagan and G. Sivashinsky, *Flame propagation and extinction in large-scale vortical flows,* Combust. Flame **120**, 222 (2000)

[31] L. Kagan, P.D. Ronney and G. Sivashinsky, *Activation energy effect on flame propagation in large-scale vortical flows,* Combust. Theory Modelling **6**, 479 (2002).

[32] Ya. Kanel, *Stabilization of solutions of the Cauchy problem for equations encountered in combustion theory*, Mat. Sbornik, **59**, 1962, 245-288.

[33] A. Kerstein, *Simple derivation of Yakhot's turbulent premixed flamespeed formula,* Combust. Sci. Tech. **60**, 163 (1988).

[34] A. Kerstein, W.T. Ashurst and F.A. Williams, *Field equation for interface propagation in an unsteady homogenous flow field,* Phys. Rev. A, **37**, 2728 (1988).

[35] A. Kiselev and L. Ryzhik, *Enhancement of the travelling front speeds in reaction-diffusion equations with advection*, Ann. Inst. H. Poincaré Anal. Non Linéaire **18** (2001), no. 3, 309–358.

[36] A.N. Kolmogorov, I.G. Petrovskii and N.S. Piskunov, *Étude de l'équation de la chaleurde matière et son application à un problème biologique,* Bull. Moskov. Gos. Univ. Mat. Mekh. **1** (1937), 1-25. (see [38] pp. 105-130 for an English transl.)

[37] A. Majda and P. Souganidis, *Large scale front dynamics for turbulent reaction-diffusion equations with separated velocity scales,* Nonlinearity, **7**, 1994, 1-30.

[38] Dynamics of curved fronts, P. Pelcé, Ed., Academic Press, 1988.

[39] N. Peters, *Turbulent Combustion,* Cambridge University Press, Cambridge, UK 2000.

[40] T. Poinsot, D. Veynante and S. Candel, *Twenty-Third Symposium (International) on Combustion*, The Combustion Institute , p. 613 (1990).

[41] P.B. Rhines and W.R. Young, *How rapidly is a passive scalar mixed within closed streamlines,* J. Fluid Mech. **133** (1983).

[42] P.D. Ronney, *Some open issues in premixed turbulent combustion,* in Modelling in Combustion Science, pp. 3-22, Eds. J. Buckmaster and T. Takeno (Springer-Verlag Lecture Notes in Physics, 1994).

[43] J.-M. Roquejoffre, *Stability of travelling fronts in a model for flame propagation II*, Arch. Rat. Mech. Anal. **117**, 1992, 119-153.

[44] J.-M. Roquejoffre, *Eventual monotonicity and convergence to travelling fronts for the solutions of parabolic equations in cylinders*, Annal. Inst. Poincare, Analyse Nonlinéare, **14**, 1997, 499-552.

[45] M.N. Rosenbluth, H.L. Berk, I. Doxas and W. Horton, *Effective diffusion in laminar convective flows,* Phys. Fluids **30**, p. 2636 (1987).

[46] B. Shraiman, *Diffusive transport in a Rayleigh-Bénard convection cell,* Physical Review A **36**, p. 261 (1987).

[47] S.S. Shy, P.D. Ronney, S.G. Buckley and V. Yakhot, *24th International Symposium on Combustion,* Combustion Inst., Pittsburgh, 1992, p. 543.

[48] G.I. Taylor, Proc. R. Soc. London Ser A **219** p. 189 (1953).

[49] A. Volpert, V. Volpert and V. Volpert, *Travelling Wave Solutions of Parabolic Systems,* Translations of mathematical Monographs, **140**, Amer. Math. Soc., Providence, Rhode Island 1994.

[50] F.A. Williams, *Combustion Theory*, ed. Benjamin Cummings (1985).

[51] J. Xin, *Existence of planar flame fronts in convective-diffusive periodic media,* Arch. Rat. Mech. Anal., **121**, 1992, 205-233.

[52] J. Xin, *Existence and nonexistence of travelling waves and reaction-diffusion front propagation in periodic media,* Jour. Stat. Phys., **73**, 1993, 893-926.

[53] J. Xin, *Analysis and modelling of front propagation in heterogeneous media,* SIAM Rev. 42 (2000), no. 2, 161–230

[54] N. Vladimirova and R. Rosner, *Model flames in Boussinesq limit: The effects of feedback,* in preparation.

[55] V. Yakhot, *Propagation velocity of premixed turbulent flames,* Combust. Sci. Tech. **60**, 191 (1988).

[56] W. Young, A. Pumir and Y. Pomeau, *Anomalous diffusion of tracer in convection rolls,* Phys. Fluids A **1**, p. 462 (1989).

[57] Ya.B. Zeldovich, G.I. Barenblatt, V.B. Librovich and G.M. Makhviladze, *The Mathematical Theory of Combustion and Explosions,* Translated from the Russian by Donald H. McNeill. Consultants Bureau [Plenum], New York, 1985.